Heliyon 9 (2023) e19998

Contents lists available at ScienceDirect

Heliyon

journal homepage: www.cell.com/heliyon

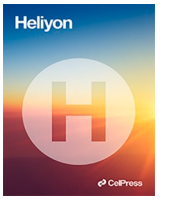

# Analysis of spatiotemporal variations and influencing factors of soil erosion in the Jiangnan Hills red soil zone, China

Fuyin Guo [a,1], Xiaohuang Liu [b,c,1], Zulpiya Mamat [a,*], Wenbo Zhang [b,c], Liyuan Xing [b,c], Ran Wang [b,c], Xinping Luo [b,c], Chao Wang [c], Honghui Zhao [c]

[a] College of Geography and Remote Sensing Sciences, Xinjiang University, Urumqi, 830000, China
[b] Key Laboratory of Natural Resource Coupling Process and Effects, Beijing, 100055, China
[c] Natural Resources Comprehensive Survey Command Center, China Geological Survey, Beijing, 100055, China

ARTICLE INFO

*Keywords:*
Soil erosion
RUSLE model
Spatial and temporal evolution
Regression analysis
GeoDetector

ABSTRACT

Soil erosion is an important environmental problem in China. The hilly region of Jiangnan is characterized by severe soil erosion due to its unique climate and intensive human activities. Therefore, assessing soil erosion in this area is of great significance for achieving regional sustainable development. Based on the spatial zoning of natural resources and the spatial differences in precipitation, land cover, topographic features, and soil texture, we estimated soil erosion from 2000 to 2020 using the Revised Universal Soil Loss Equation (RUSLE) model. The study showed that micro-erosion dominates spatially in the subtropical forest subzone of the eastern hills, accounting for more than 60% of the total erosion area. Intense erosion was found in woodlands and grasslands and the erosion intensity tended to be lower in the plains. Erosion occurred mainly in areas with slopes >8°. The areas with significantly lower erosion were mainly distributed at the boundaries between forests, arable land, and artificial land surfaces. The areas where soil erosion significantly increased over the study period were mainly found in farmland areas (31.70%). Soil erosion occurred because of a combination of factors, among which vegetation cover played a prominent role. Elevation and slope were correlated with soil erosion intensity. Severe erosion in different parts of the study area showed two trends of spatial aggregation and discrete distribution. This analysis of soil erosion in the study area by the RUSLE model provides reference data for the eastern subtropical forest subregion including the Jiangnan Hills.

## 1. Introduction

Soil erosion is the spatial displacement of soil or the soil-forming matrix under the action of external forces such as water or wind [1]. Soil erosion can lead to soil degradation and exacerbates catastrophic natural disasters such as floods and mudslides, posing a threat to the sustainable development of human societies [2,3]. The sustainable development of human society is adversely affected by various types of soil erosion–such as water erosion, wind erosion and freeze-thaw erosion [4]. According to an EU monitoring report on progress towards the Sustainable Development Goals (SDGs) in the EU context, 2.01 × 105 $km^2$ of the world's land is at risk of severe soil erosion, which will seriously affect global sustainable development [5]. Therefore, it is necessary to monitor the rate of soil erosion

* Corresponding author.
*E-mail addresses:* yinfunan@163.com (F. Guo), liuxh19972004@163.com (X. Liu), haonidd@nuaa.edu.cn (Z. Mamat).
[1] Equal contributions.

https://doi.org/10.1016/j.heliyon.2023.e19998
Received 3 July 2023; Received in revised form 7 September 2023; Accepted 7 September 2023
Available online 9 September 2023

dynamically as well as to determine the intensity of soil erosion [6].

Soil erosion is an important indicator in the evaluation of land degradation. There are four main soil erosion research methods: runoff plots [7], isotope tracking [8], model simulation [9], and methods based on a geographic information system (GIS) or remote sensing (RS) [10]. Researchers have developed a series of soil erosion models, including the Water Erosion Prediction Project (WEEP) [11], the Limburg Soil Erosion Model (LISEM), and the European soil erosion model (EROSION), etc. [12]. Many empirical and statistical models are based on the United States Department of Agriculture (USDA) model proposed by the Universal Soil Loss Equation (USLE) and Revised Universal Soil Loss Equation (RUSLE) [13]. The RUSLE model is based on definite factors and can be combined with mathematical and statistical methods to identify the soil erosion status of a study area. It has been widely used due to its convenient data acquisition and high accuracy [14]. At present, RUSLE models can be divided into three categories according to different research objectives: hydrological basin-oriented [15], natural terrain-oriented [16], and administrative areas [17,18]. Previous research based on the RUSLE model has mainly been conducted at small scales but with the development of 3 S technology, large-scale research is now occurring [19], e.g., on the Loess Plateau [20]. For example, Chen et al. [21]. Studied soil erosion in Hunan, Jiangxi, Zhejiang, and Fujian Provinces including the Jiangnan Hills. Despite the advances made in soil erosion research, the study of long-term changes in erosion processes still poses significant challenges.

China's swift economic and social growth has intensified the pressure on its ecology and environment. Although the Chinese government invests substantially in soil erosion control, the country still suffers from serious soil erosion [22]. Due to their subtropical climate, undulating terrain and intensive human activities, the Jiangnan Hills have become a typical water erosion area in China [23]. A comprehensive analysis of soil erosion in the hilly areas of Jiangnan is essential for managing water erosion areas and protecting the environment in the context of constructing an ecological civilization. We applied the RUSLE model in this study to assess the spatiotemporal patterns of soil erosion in the subtropical forest subregion of the eastern Jiangnan hills. The aim of the study was to assess the spatial distribution of soil erosion in the region, as well as its development trends and driving forces, and to provide a basis for developing soil and water conservation measures that are adapted to local conditions.

## 2. Materials and methods

### 2.1. Study area and data

#### 2.1.1. Overview of the study area

The subtropical forest subregion of the Jiangnan Hills is located in the eastern region, south of the Yangtze River, covering western

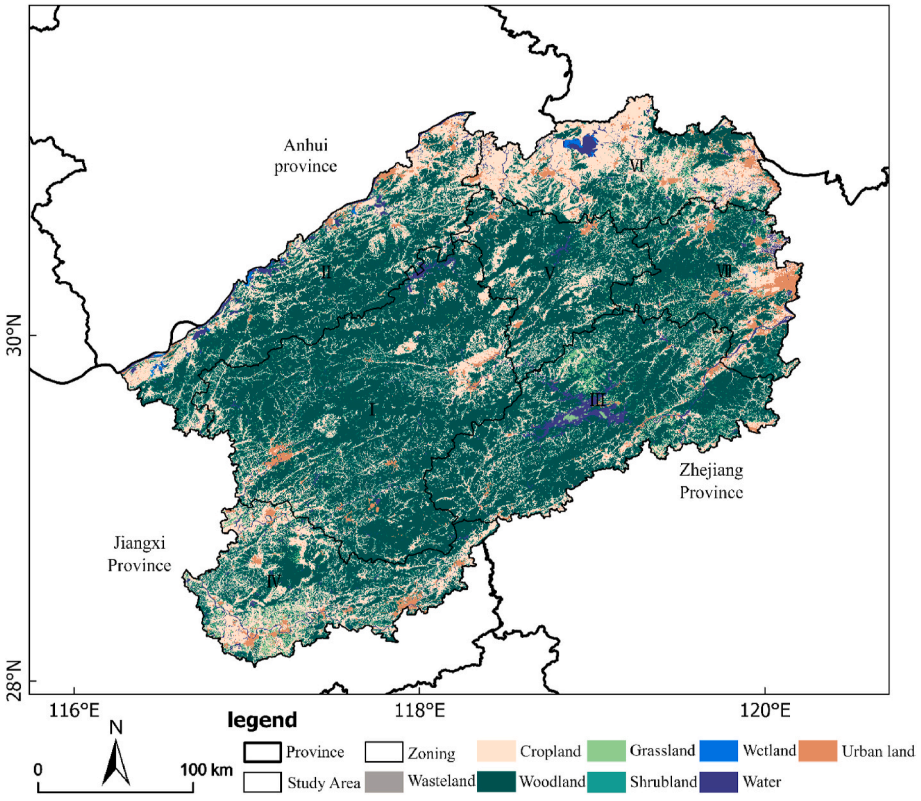


**Fig. 1.** Geographical location of the eastern subtropical forest subregion of the Jiangnan Hills.

Zhejiang Province and eastern Jiangxi Province (116°16′–120°13′E, 28°4′–31°23′N; Fig. 1). The topography of the study area is mainly mountainous and hilly with plains. The Qiandao Lake Reservoir is the largest water body in the area. The study area has a subtropical monsoon climate, with an annual average temperature of 16–20 °C; the average temperature of the coldest month is 3–9 °C. The annual precipitation is 1300–1800 mm, with the most precipitation in May and June and the least in July and August. Runoff reaches 1000 mm in mountainous areas and 800 mm in hilly and basin areas. The natural vegetation is dominated by evergreen broad-leaved trees with vines and epiphytes. Evergreen ferns and rhododendron shrubs are distributed in the forest understory or on unforested slopes. According to the Food and Agriculture Organization (FAO) soil classification system, the soils in the study area are predominantly Acrisols, and they have organic matter content ranging from 1% to 5%. The soil is sticky and poorly permeable. Because of their richness in iron and aluminum oxides, the soil shows a red color, which is collectively referred to as a red soil zone in this study. The region is densely populated, with intensive economic activities, and is an important agricultural area in China [24]. Soil erosion is a serious problem in this region due to the high temperature and rainfall, the easily eroded red soil, and the intensive agricultural activities.

The boundary delineation of the eastern subtropical forest subregion of the Jiangnan hills is based on the natural resource element observation projects of the Geological Survey of China, Ministry of Natural Resources [25,26]. The study classifies China into various resource regions according to the spatial patterns of natural resource elements [27]. The study area is the eastern subtropical forest subregion of the Jiangnan hills, which has an area of 79,270 $km^2$ and comprises seven resource zones. The seven resource zones are: (I) the subtropical coniferous forest zone in the northwest of Shangrao City, (II) the water-dry crop and scrub planting zone in the south of Wuhu City, (III) the dry crop planting zone in the northwest of Quzhou City, (IV) the tropical grass zone in the south of Jingdezhen City, (V) the deciduous broadleaf scrub zone in the northeast of Huangshan City, (VI) the water-dry rotation plantation zone in the west of Huzhou City, and (VII) the coniferous forest and water-dry rotation plantation zone in the southwest of Huzhou City.

#### *2.1.2. Data*

The data included a digital elevation model (DEM), precipitation data, land use data, vegetation cover data, and soil texture data. The specific data sources are shown in Table 1. The DEM was downloaded in the geospatial data cloud and 90 m resolution data were synthesized. Annual Normalized Difference Vegetation Index (NDVI) data for China were generated by the maximum synthesis method based on continuous time series data (1990–2020) from SPOT/VEGETATION NDVI satellite remote sensing data. Soil composition data were obtained from the World Soil Database constructed by the Food and Agriculture Organization of the United Nations (FAO) and the International Institute for Applied Systems (IIASA) in Vienna. The NDVI and land use data were selected for 2000, 2005, 2010, 2015, and 2020.

### *2.2. Research methodology*

#### *2.2.1. The RUSLE model*

The basic form of the RUSLE model (Equation (1)) is:

$$A = R \times L \times S \times C \times P \times K \tag{1}$$

where $A$ is the annual soil erosion per unit area calculated by the model in t/($km^2$ ·a). $R$ is the rainfall erosion force factor in MJ·mm/($hm^2$·h·a), which is the dynamic index of soil erosion caused by precipitation runoff [28]. $L$ is the slope length factor, which is normalized to 22.13 m slope length. $S$ is the slope factor, which is normalized to a slope factor of 5.14° [29]. $K$ is the soil erosion factor in t·$hm^2$·h/($hm^2$·MJ·mm), which reflects the ease of soil particles being hydraulically separated and transported [30]. $C$ is the vegetation cover factor, which is dimensionless and indicates the effect of different types of vegetation cover on soil conservation and soil erosion [31]. The $P$ factor is the soil and water conservation measure factor, which is dimensionless, and represents the ratio of soil loss under soil and water conservation measures to soil loss under slope planting [32].

#### *2.2.2. Rainfall erosion force factor (R)*

Rainfall erosion force reflects the ability of rainfall to cause soil erosion. Its magnitude is related to rainfall amount, rainfall intensity, nature of the subsurface, raindrop size, and the speed of the falling end point [33]. Combining the natural surface of the mountainous hills in the study area, as well as climatic factors, this paper uses the method proposed by Zhang [34] was used to

**Table 1**
Study data.

| Data | Resolution | Format | Source |
|---|---|---|---|
| DEM: Digital Elevation Model | 90 m | FGDBR | Geospatial Data Cloud (https://www.gscloud.cn/) |
| 2000–2020 precipitation dataset Rainfall data | 1 km | TIFF | National Science and Technology Infrastructure Platform–National (http://www.geodata.cn/) |
| 2000–2020 Land Cover Data LUCC | 1 km | TIFF | Earth System Science Data Center Data Center for Resource and Environmental Sciences, Chinese Academy of Sciences (https://www.resdc.cn/) |
| 2000–2020 NDVI; Annual Vegetation Index of China | 1 km | TIFF | Data Center for Resource and Environmental Sciences, Chinese Academy of Sciences (https://www.resdc.cn/) |
| Soil texture data | 875 m | TIFF | Food and Agriculture Organization of the United Nations (https://www.fao.org/) |

calculate the *R*-factor (Equation (2)) of precipitation erosion force based on annual precipitation:

$$R = \alpha_1 P^{\beta_1} \tag{2}$$

where *P* is the average annual rainfall (mm); *R* is the average multi-year rainfall erosion force in MJ· mm/(hm$^2$·h·a); and $\alpha_1$, and $\beta_1$ are model parameters ($\alpha_1 = 0.0534$, $\beta_1 = 1.6548$).

### 2.2.3. Vegetation cover factor (C)

The *C*-factor (Equation (3)) is a characterization of vegetation features, such as vegetation type, vegetation combination, tillage method, productivity level, growing season length, crop residue management, and other factors that affect soil erosion [35]. The *C*-value ranges from 0 to 1. When the *C*-value is 1, the ground is completely bare without vegetation; when the *C*-value is close to 0, the ground is well-vegetated. Previous studies have shown that there is a quantitative relationship between vegetation cover and soil erosion [36]. In this paper, the calculation of the *NDVI* followed the method (Equation (4)) of Almagro et al. [37]. Vegetation cover (fg) (Equation (5)) was calculated by an image dichotomous approach [38,39]:

$$C = \begin{cases} 1 & f_g = 0 \\ 0.6508 - 0.3436 \lg f_g & 0 < f_g \leqslant 78.3\% \\ 0 & f_g > 78.3\% \end{cases} \tag{3}$$

$$NDVI = (Band4 - Band3)/(Band4 + Band3) \tag{4}$$

$$f_{\text{fl}} = (NDVI - NDVI_{min}) \,/\, (NDVI_{\max} - NDVI_{min}) \tag{5}$$

where $NDVI_{min}$ denotes *NDVI* minimum and $NDVI_{max}$ denotes *NDVI* maximum. *Band3* denotes the infrared band and *Band4* denotes the near-infrared band.

### 2.2.4. Soil and water conservation measures factor (P)

The *P*-factor in the RUSLE model can be determined experimentally with high accuracy in small watershed studies. The *P*-factor is rarely considered in large-scale soil erosion risk modeling [28]. The *P*-factor is the ratio of soil erosion under a specific soil conservation measure to soil erosion when the corresponding downward slope planting without the conservation measure is implemented [40]. In practice, soil conservation measures reduce soil erosion by reducing the rate of surface runoff [41]. Therefore, the stronger the surface protection measures, the smaller the *P*-value is; when the *P*-value is 0, soil erosion will not occur. Combining the current land use in the study area and previous experience, the *P* values are shown in Table 2 (major soil and water conservation farming measures in China).

### 2.2.5. Slope and slope length topographic factors

We use the slope (*S*) factor and slope length (*L*) factor (Equation (6)) instead of topographic features in the study area. The size of the raster affects the extraction of topographic factors. Too small a raster image element will interfere with the calculation of the ground cover; too large a grid will make the slope calculation smaller. We use raster data with 90 m spatial resolution. The slope length factor normalized to the 22.13 m slope length was used in the RUSLE model [42,43]. The expression is:

$$L = (\lambda/22.13)^m \tag{6}$$

Where $\lambda$ is the projected length of the grid cell, *L* is the soil erosion normalized by the slope length of 22.13 m, and m is the slope length factor index.

The *S*-factor (Equation (7)) in the CLSE [44]model is calculated separately for different slopes:

$$S = \begin{cases} 10.8 \sin\theta + 0.03 & \theta \leqslant 5^\circ \\ 16.8 \sin\theta - 0.5 & 5^\circ < \theta < 10^\circ \\ 21.97 \sin\theta - 0.96 & \theta \geqslant 10^\circ \end{cases} \tag{7}$$

### 2.2.6. Soil erosion factor

The soil erosion coefficient *K* is a measure of soil resistance to erosion and reflects the soil's sensitivity to erosion. Liu proposed a soil erosion index, taking into account national conditions [45]. Williams et al. [46]. Proposed a more concise estimation method for the *K*-factor (Equation (8)) in the Erosion Productivity Impact Calculator (EPIC) model:

**Table 2**
P-values of different land use types.

| Projects | Dryland | Water Field | Forest | Grassland | Waters | Urban and Rural Land | Swamp | Bare ground |
|---|---|---|---|---|---|---|---|---|
| P | 0.55 | 0.25 | 0.9 | 0.9 | 0 | 0 | 0 | 1 |

$$K = 0.1317\left\{0.2 + 0.3\exp\left[-0.0256SA\left(1 - \frac{SI}{100}\right)\right]\right\} \times \left(\frac{SI}{CL + SI}\right)^{0.3} \times \left[1.0 - \frac{0.25C}{C + \exp(3.72 - 2.95C)}\right] \times \left[1.0 - \frac{0.7SAI}{SA1 + \exp(-5.51 + 22.9SAI)}\right] \tag{8}$$

where $K$ denotes the soil erosion factor, $SAI$ equals 1-$SA$/100; $SA$ is the powder content (%); $SI$ is the clay content (%); $CL$ is the sand content (%); and $C$ denotes the soil organic carbon content (%).

### 2.3. Analysis

#### 2.3.1. Zoning statistics

The soil erosion degree in the study area was classified into six grades: micro, slight, moderate, intense, extremely intense, and severe, according to the Soil Erosion Classification and Grading Standard (SL190-2007) issued by the Ministry of Water Resources of the People's Republic of China. According to the comprehensive natural resources zoning program [25], soil erosion was analyzed for each of the seven resource zones within the eastern subtropical forest subzone of the Jiangnan Hills. Following Cui et al. [47]., we divided the slope of the study area into six classes (Fig. 2): 0°–5°, 5°–8°, 8°–15°, 15°–25°, 25°–35°, and 35°–90°. The spatial distribution relationship between soil erosion and land use types was examined for different land use types.

#### 2.3.2. Trend analysis

The interannual soil erosion raster layers were subjected to one-dimensional regression in a time series to investigate the interannual trend of soil erosion. The regression coefficient was calculated using the least squares method (Equation (9)) with time the $X$-axis and value as the $Y$-axis. A positive slope indicated an increase in soil erosion and a negative slope indicates a decrease in soil erosion. The expressions were as follows:

$$\theta_{\text{slope}} = \frac{n \times \sum_{i=1}^{n} i \times A_i - \sum_{i=1}^{n} i \sum_{i=1}^{n} A_i}{n \times \sum_{i=1}^{n} i^2 - \left(\sum_{i=1}^{n} i\right)^2} \tag{9}$$

where $\theta_{slope}$ denotes the slope of the regression equation, $n$ denotes the year, and $A_i$ denotes the annual soil erosion. The $F$ test (Equation (10)) was applied as follows:

$$F = \frac{SSR/K}{SSE/(n - K - 1)} \tag{10}$$

where SSR is the regression sum of squares, calculated by $\Sigma_{i=1}^{n}(\hat{y} - \overline{y})^2$. $SSE$ is the residual sum of squares, calculated by $\Sigma_{i=1}^{n}(\hat{y} - y_i)^2$, where $\hat{y}$ is the regression fitted value of annual soil erosion, $\overline{y}$ is the mean of annual soil erosion data, and $y_i$ is the true value of annual

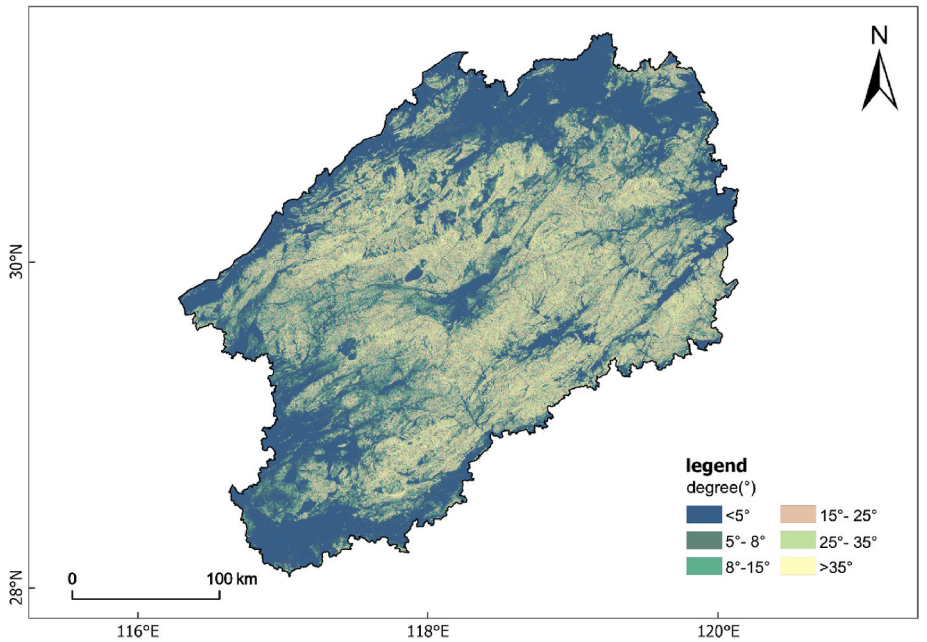


**Fig. 2.** Slope map of the study area.

soil erosion data, and $K$ represents the number of independent variables (1 in this paper). The significance test results were classified into five levels by $F$ value and significance level $\alpha$, which are a highly significant increase ($\theta_{slope} > 0$, $\alpha < 0.01$), significantly increased ($\theta_{slope} > 0$, 0.01, $\alpha < 0.05$), insignificant ($\alpha > 0.05$), significantly decreased ($\theta_{slope} < 0$, 0.01, $\alpha < 0.05$), and highly significantly decreased ($\theta_{slope} < 0$, $\alpha < 0.01$).

#### 2.3.3. Driving forces of soil erosion

GeoDetector is a statistical method proposed by Wang to quantitatively assess the stratified heterogeneity [48]. GeoDetector can be used to explore the explanatory power of the independent variable ($X$) on the dependent variable ($Y$) [49]. We conducted a factor-probe analysis of soil erosion ($Y$) and 12 explanatory factors ($X$) to explore the main drivers. The method (Equation (11)) uses q values to measure the extent to which factor $X$ explains the spatial variation of the attribute $Y$ [50]:

$$q = 1 - \frac{\sum_{h=1}^{L} N_h \sigma_h^2}{N\sigma^2} = 1 - \frac{SSW}{SST} \tag{11}$$

$$SSW = \sum_{h=1}^{L} N_h \sigma_h^2, SST = N\sigma^2 \tag{12}$$

where $L$ is the stratification of variable $Y$ or independent variable $X$; $N_h$ and $N$ are the numbers of stratum $h$ and area cells, respectively; $\sigma_h^2$ and $\sigma^2$ are the variance of $Y$ values in stratum h and the whole area, respectively; $SSW$ and $SST$ (Equation (12)) are the sums of the variance within a stratum and the total variance of the whole area, respectively.

## 3. Results

### 3.1. Temporal variation

The total soil erosion in the study area in 2000, 2005, 2010, 2015, and 2020 (Fig. 3) was $1.07 \times 10^8$, $9.86 \times 10^7$, $1.02 \times 10^8$, $7.34 \times 10^7$, and $6.74 \times 10^7$ t/a, respectively. The erosion volume increased slightly in 2010 but there was a significant overall decreasing trend ($P < 0.05$). In 2020, compared with 2000, the amount of soil erosion had decreased by 37.14%.

#### 3.1.1. Spatial and temporal variation under different zoning

Table 3 shows that the overall soil erosion of each seven resource zones decreased from 2000 to 2020 (Fig. 4). The study area's average soil erosion modulus reached its highest point in 2010. The total soil erosion of the three resource zones II, IV, VII decreased and then increased from 2000 to 2010. The total soil erosion and the proportion of the eroded area graded moderate and above in Zone III decreased. Overall, the soil erosion intensity was highest in zone III, followed by zones I, IV, II, VII, and V, and was lowest in plot VI.

#### 3.1.2. Spatial and temporal variation of soil erosion under different land uses

As can be seen from Fig. 5, micro erosion and slight erosion dominated during the 20 years, i.e., >70% of erosion occurrence in each land use type. Intense and above-level erosion was concentrated in woodlands and grasslands. Among different land use types, the area of micro and slight erosion occurring on cropland accounts for more than 92.84% of the area of cropland, which is the highest proportion among the six land use types. Forest land is the most widely distributed in the study area, with an area of 50,420 km$^2$, accounting for 65.03% of the study area. For 2000, 2005, 2010, 2015, and 2020, the area of forest land with moderate and above erosion

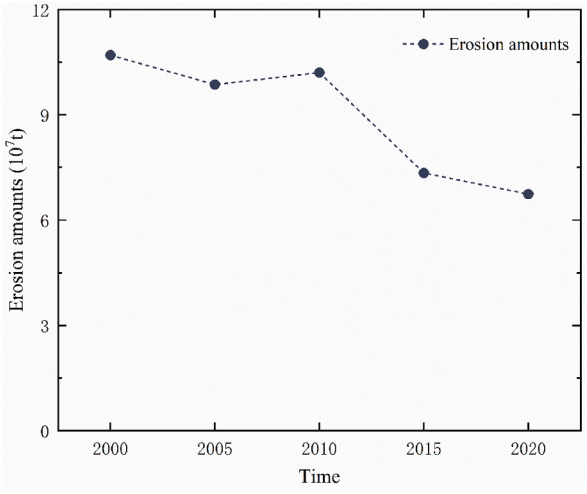


**Fig. 3.** Total soil erosion in the study area.

**Table 3**
Soil erosion status of the subtropical forest subregion in the eastern Jiangnan Hills **2000–2020**.

| Year | resource zone | Average soil erosion modulus [t/(km$^2$ · a)] | Soil erosion volume ($10^6$ t/ · a) | Percentage of moderate and above erosion area/% |
|---|---|---|---|---|
| 2000 | I | 1292.35 | 27.02 | 19.00 |
| | II | 931.23 | 10.99 | 13.05 |
| | III | 2380.25 | 33.17 | 38.99 |
| | IV | 1627.54 | 14.80 | 21.12 |
| | V | 1282.08 | 8.76 | 20.58 |
| | VI | 495.40 | 4.20 | 4.77 |
| | VII | 1196.17 | 8.33 | 19.77 |
| 2005 | I | 1265.26 | 26.45 | 19.33 |
| | II | 735.98 | 8.68 | 10.24 |
| | III | 2119.22 | 29.53 | 36.37 |
| | IV | 1491.63 | 13.56 | 19.21 |
| | V | 1242.02 | 8.49 | 21.11 |
| | VI | 493.71 | 4.19 | 5.16 |
| | VII | 1103.48 | 7.69 | 17.85 |
| 2010 | I | 1360.30 | 28.44 | 18.44 |
| | II | 848.89 | 10.02 | 11.80 |
| | III | 1828.37 | 25.49 | 27.41 |
| | IV | 1848.50 | 16.84 | 23.72 |
| | V | 1000.64 | 6.84 | 14.99 |
| | VI | 566.24 | 4.81 | 6.28 |
| | VII | 1367.22 | 9.54 | 22.89 |
| 2015 | I | 841.92 | 17.60 | 11.42 |
| | II | 676.25 | 7.98 | 9.01 |
| | III | 1381.44 | 19.25 | 19.12 |
| | IV | 1302.87 | 11.84 | 15.64 |
| | V | 822.14 | 5.62 | 11.92 |
| | VI | 465.63 | 3.95 | 5.17 |
| | VII | 1026.13 | 7.15 | 16.06 |
| 2020 | I | 750.02 | 15.64 | 10.63 |
| | II | 498.70 | 5.86 | 6.52 |
| | III | 1255.80 | 17.54 | 18.23 |
| | IV | 1161.28 | 10.66 | 13.73 |
| | V | 930.29 | 6.34 | 14.24 |
| | VI | 476.69 | 4.00 | 4.97 |
| | VII | 1063.24 | 7.38 | 16.82 |

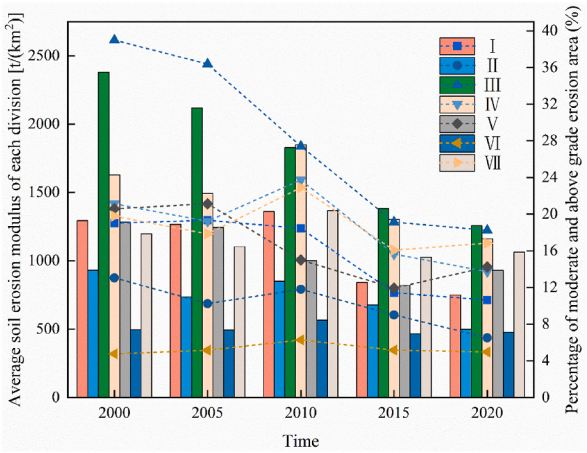


**Fig. 4.** Average modulus map of soil erosion in different seven divisions.
Note: The magnitude of erosion per unit area of soil and soil parent material per unit time is the soil erosion modulus. The histogram indicates the average soil erosion modulus within each resource zone, and the dashed line indicates the percentage of the eroded area graded moderate and above in the corresponding year.

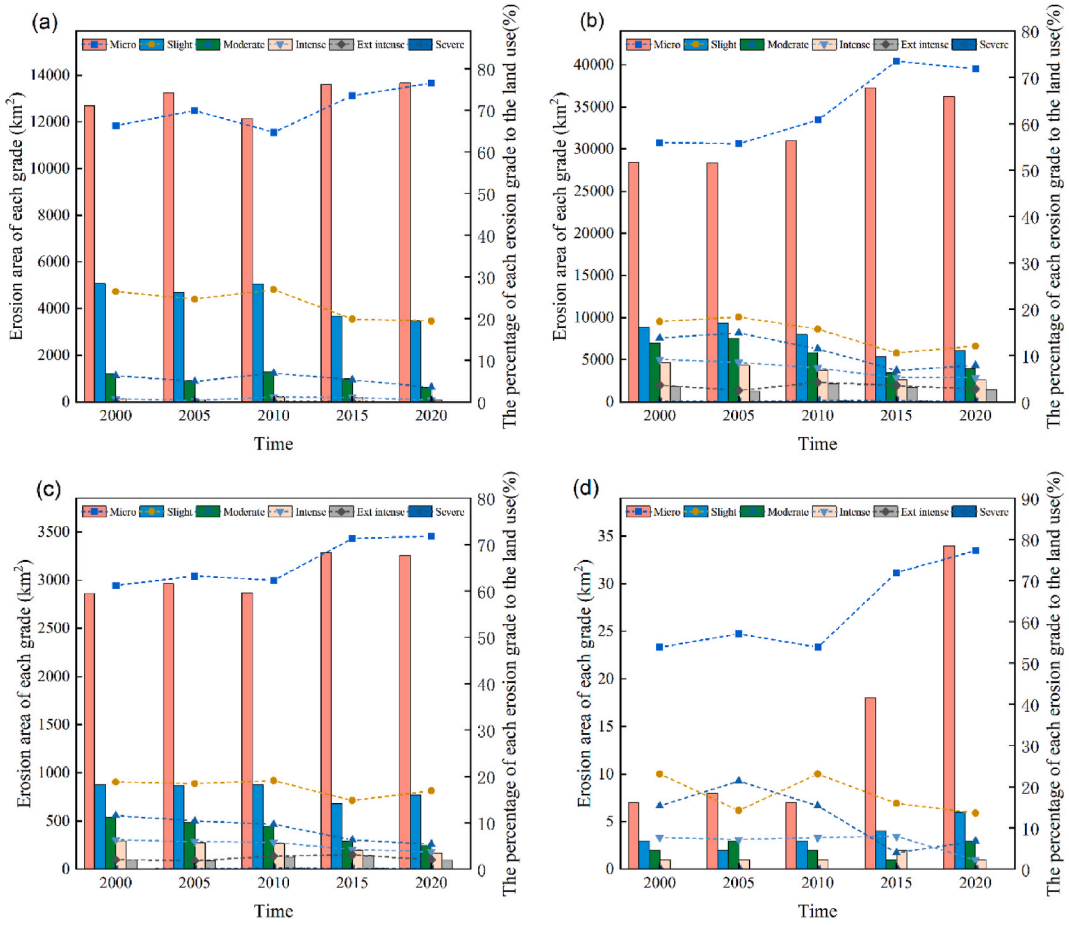


**Fig. 5.** Temporal variations of soil erosion grades at different land use types: (a) cropland, (b) woodland, (c) grassland, and (d) wasteland from 2000 to 2020.

Note: The area of different erosion classes, and the line indicates the percentage of that class of erosion to the area of the corresponding land use pattern.

is 13,614, 13,231, 11,966, 8051, and 8106 km$^2$, accounting for 26.73%, 26.00%, 23.49%, 15.87%, and 15.87% of the study area, respectively. The area and proportion of grassland experiencing moderate or above soil erosion were second only to forests, with an area of 510, 637, 856, 854, and 936 km$^2$, with area proportions of 20.00%, 18.24%, 18.58%, 13.83%, and 11.24%, respectively. The grassland use type is smaller in area and its soil erosion trend is similar to that of forests. The land use patterns of partial natural vegetation types are consistent with the regional erosion changes.

### *3.1.3. Spatial and temporal variation characteristics of soil erosion under different slopes*

As can be seen from Fig. 6, the area of micro erosion in each slope class was the largest. The intensity of soil erosion decreases at each slope class, and the steeper the slope, the greater the proportion of area where stronger erosion is transformed to micro erosion. The intensity of soil erosion decreases at each slope class, and the steeper the slope, the greater the proportion of area where stronger erosion is transformed to micro erosion. The proportion of erosion occurrence under the same erosion intensity is positively correlated with slope. Slight erosion was mainly concentrated from 0° to 8°, moderate erosion 5°–15°, intense erosion 8°–25°, extremely intense erosion 15°–35°, and intense erosion 25°–90°. The areas with a slope >8° should be the soil erosion management focus. Over the study period, the average area of micro erosion was 47,103, 47,956, 49,718, 58,375, and 58,236 km$^2$, with average percentages of 63.83%, 61.11%, 65.39%, 76.83%, and 77.77%, respectively. The trend was increasing and the soil erosion condition improving. Micro erosion increased by 22.74% in the 25°–35° slope class, 14.38% in the 5°–8° slope class, 10.85% in the 15°–25° slope class, 8.36% in the 25°–35° slope class, and 8.36% in the extremely intense erosion class. The area of extremely intense erosion increased by 5.42% in the 35°–90° slope class and the area of severe erosion increased by 1.46% in the 35°–90° slope class. When the slope grade was <5°, the soil erosion condition was more stable. As the slope grade increased, there was no obvious correlation between soil erosion condition recovery and slope grade. The more serious the soil erosion condition, the smaller the degree of change.

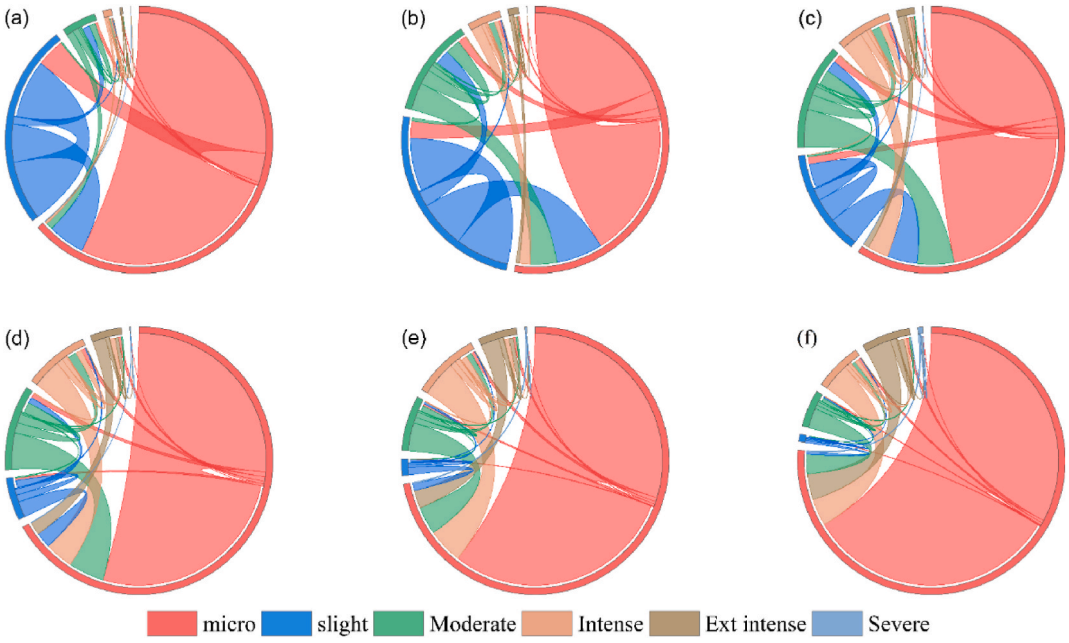


**Fig. 6.** Temporal variations of soil erosion grades at different slopes: (a) 0–5°, (b) 5–8°, (c) 8–15°, and (d) 15–25°, (e) 25–35°, and (f) 35–90° from 2000 to 2020.

### *3.1.4. Erosion changes for the major land use types in steep slope areas*

The statistical characteristics of the occurrence of soil erosion graded as moderate and above were analyzed for arable land, forest land, and grassland when the slope was >15° (Fig. 7). The largest area of erosion occurred on forest land with an average erosion area of 5293.4 km$^2$, accounting for 10.41% of the erosion area of this land use. This should be the focus of soil erosion management in the study area. The average erosion area on cropland was 2126.2 km$^2$ and grassland was 2024.2 km$^2$. The average erosion area on cropland was 5.04% higher than the average erosion area on grassland, but the eroded area graded moderate and above on cropland was 34.13%, which was higher than that on grassland. Soil erosion of moderate and above grade in three land use types (forest land, cropland, and grassland) decreased over the study period. The erosion area of forest land decreased by 2892 km$^2$, a decrease of 60.21%. The erosion area of cropland decreased by 66.22%, which represented the largest decrease. There was a clear improvement in soil erosion graded as moderate and above on steep slopes in the study area for the main land use types.

### *3.1.5. Distribution characteristics of soil erosion of intense and above grades*

Fig. 8 shows that erosion centers were concentrated in the central and southwestern parts of the study area. Using a hot spot (Getis-

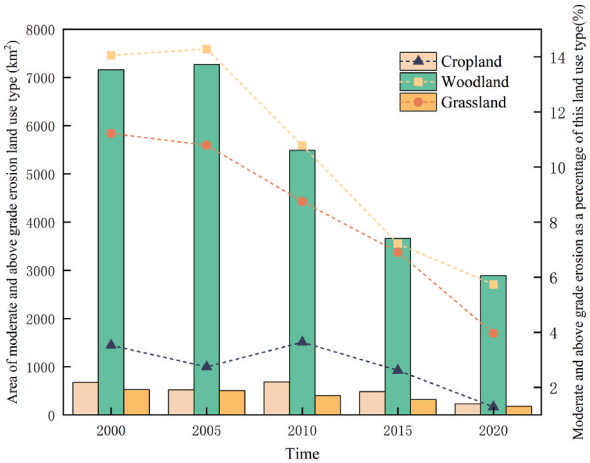


**Fig. 7.** Soil erosion maps of different land use types on steep slopes.
Note: The area of moderate and above grade erosion of different land use types with the dashed line indicating the percentage of erosion area in this land use pattern.

Ord Gi*) algorithm to determine the spatial distribution of eroded areas graded as strong and above in the study area, it was found that these areas in zones I, III, IV, and V showed a significant spatial clustering ($P < 0.05$). The spatial distribution of eroded areas graded as intense and above in zones II, VI, and VII was discrete ($P < 0.05$). The eroded areas graded as intense and above in the study area decreased over time. The central and southwestern parts should be the focus of soil erosion management in the study area. There was a concentration of arable land in this area with steep slopes, and therefore this land use needs to be further optimized. Slopes with serious soil erosion problems should be retired, afforested, planted with grass, or restored naturally according to the actual situation.

### 3.2. *Time series analysis of soil erosion factors in the study area*

The interannual soil erosion data, precipitation erosion force, vegetation cover, and soil conservation measures were analyzed by a

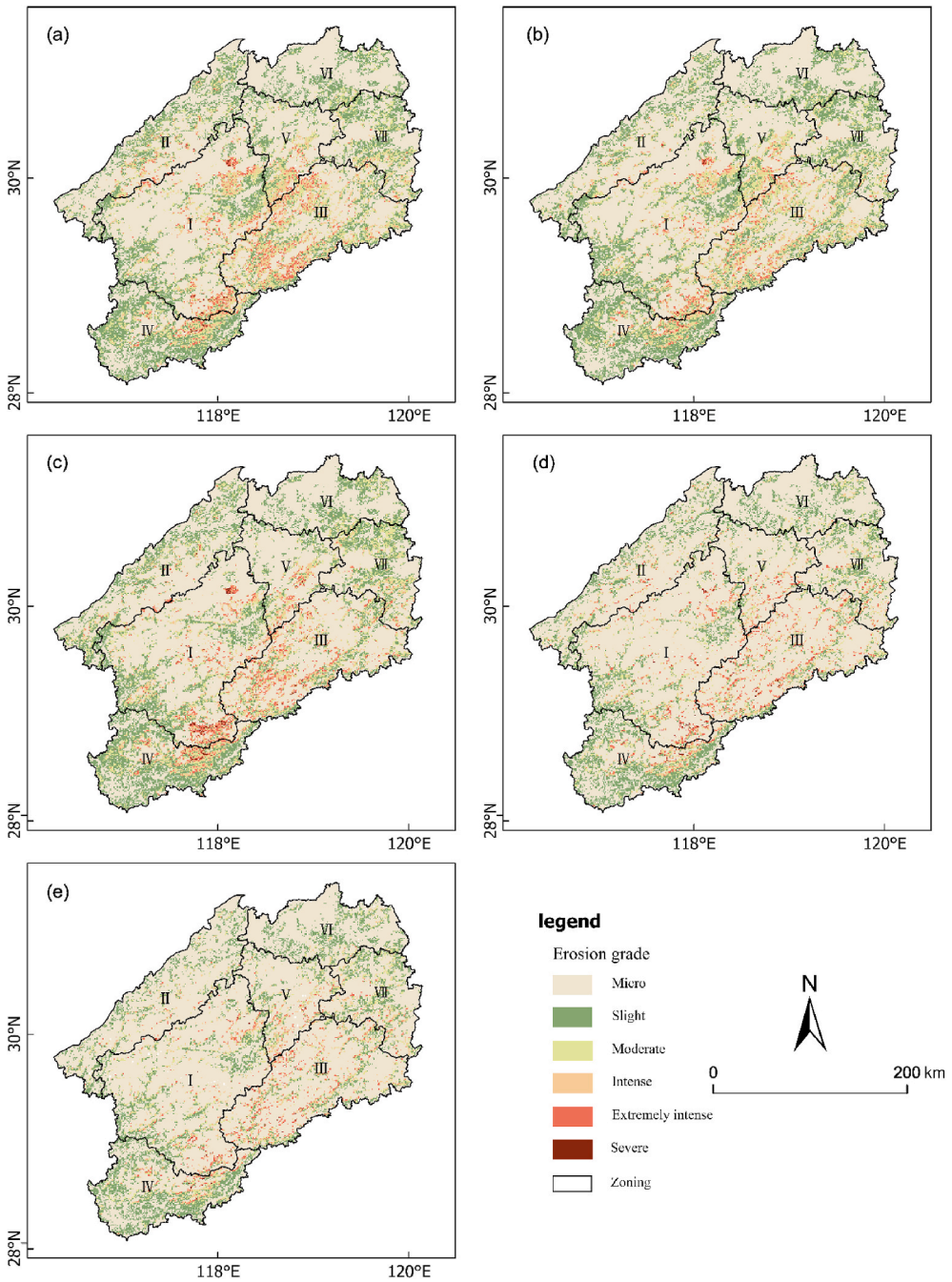


**Fig. 8.** Spatial variation of soil erosion grade in the historical period (a) 2000, (b) 2005, (c) 2010, (d) 2015, and (e) 2020.

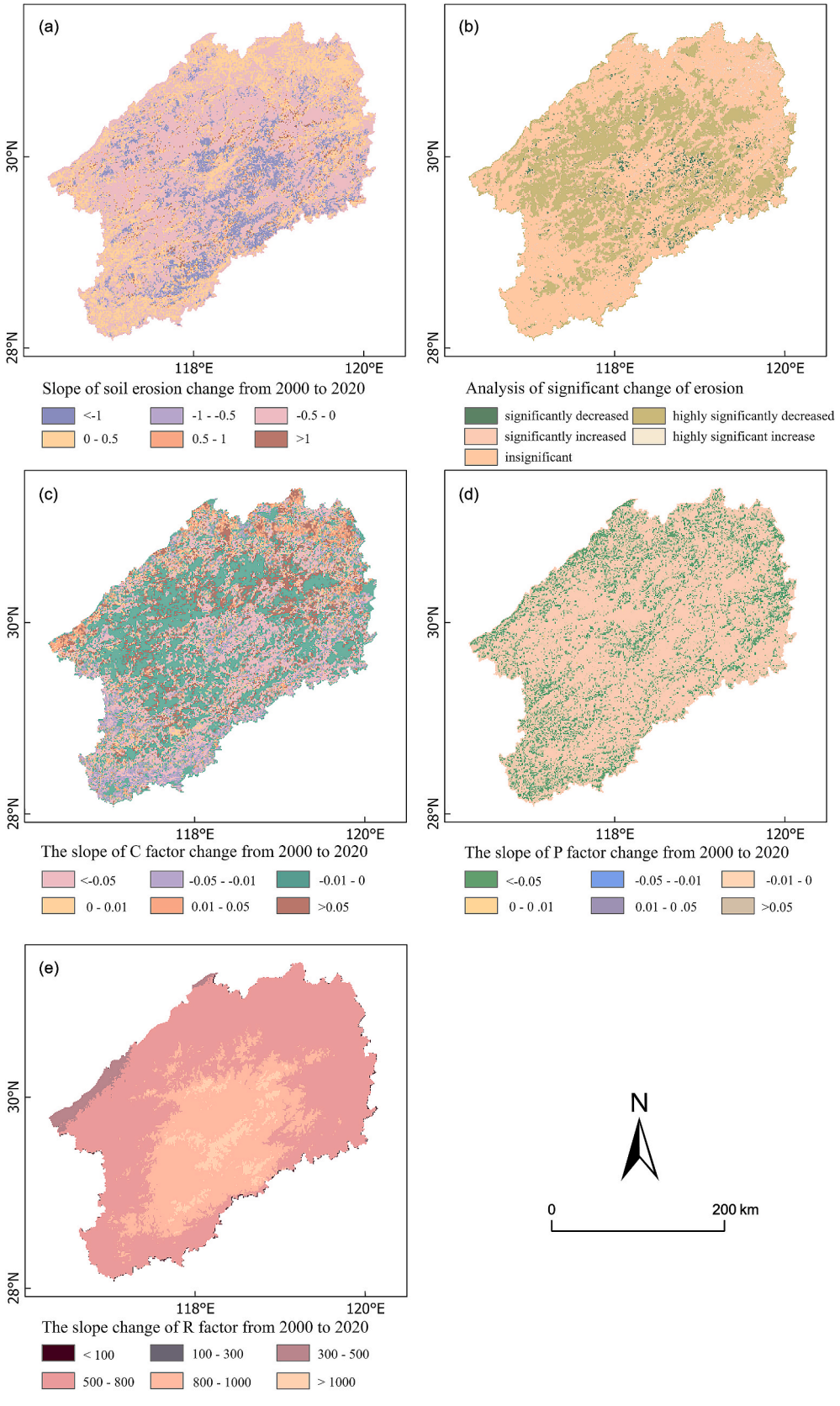


*(caption on next page)*

**Fig. 9.** Least square method results for (a) soil erosion, (c) vegetation cover factor, (d) soil and water conservation measures factor, and (e) rainfall erosion force factor, and (b) significance test of soil erosion from 2000 to 2020.
Note: The values in the graph are the coefficients of the regression equation, dimensionless.

linear regression (Fig. 9). Over the study period, 36% of the area showed a significant decrease ($P < 0.05$) in soil erosion, while 32.27% of the area maintained the same soil erosion conditions, which overlapped significantly with the *C*-factor one-way regression results in the low-value area distribution. Soil erosion in 31.70% of the area increased significantly ($P < 0.05$), with a large spatial overlap with the distribution of cultivated land. Soil erosion significantly decreased ($P < 0.05$) over an area of 1758 $km^2$, accounting for 2.22% of the study area; soil erosion significantly decreased ($P < 0.01$) over an area of 23,810 $km^2$, accounting for 30.06% of the study area; soil erosion significantly increased over an area of 296 $km^2$ ($P < 0.01$), accounting for 0.37% of the study area; soil erosion significantly increased over an area 3245 $km^2$ ($P < 0.05$), accounting for 4.10% of the study area; and there was no significant change in soil erosion over an area of 50,094 $km^2$, accounting for 63.25% of the study area. Soil erosion increased mainly in the cultivated areas, which was consistent with the earlier result that soil erosion was more likely to occur in cultivated areas than in grasslands when the slope was $>15^{\circ}$. The areas where soil erosion reduced were mainly areas of human activity and forest land, which were close to the main arable land areas. This was due to the return of farmland to forests and grassland.

In the RUSLE model, *K*, *L*, and S were constant factors and *C*, *R*, and *P* influenced soil erosion. The area with a decreasing *C*-value was widely distributed in forest land and grasslands. The area with an increasing *C*-value was mainly distributed in the northeast of the study area and border area, and in cultivated areas and mixed cultivated forest areas, in which there was an increase in vegetation cover. The change in the *C*-value was positively correlated with soil erosion mainly in cultivated land areas.

### 3.3. The driving force of soil erosion

#### 3.3.1. Detection factor univariate analysis

Geodetector was applied to show the degree of explanation (q value) of 12 factors for the occurrence of soil erosion. As shown in Table 4, the relevance ranking was land use cover change (*LUCC*) > *Precipitation* > *Population* > *GDP* > *Aspect* > *NDVI* > *Silt* > *Clay* > *Sand* > *Temperature* > *DEM* > *Slope*. The influence of each factor on the occurrence of soil erosion was balanced and the occurrence of soil erosion in the study area was influenced by a combination of factors. The land use factor had the greatest influence on the occurrence of soil erosion (0.269), and precipitation, vegetation cover, slope orientation, air temperature, sandy soil, clay, and slit influence were >0.2. The population density and gross domestic product q values were >0.24.

#### 3.3.2. Factor interaction

Fig. 10 shows that the *NDVI* ∩ *Aspect* (q value of 0.342) ranked first in terms of interactions, followed by *NDVI* ∩ *Precipitation* (q value of 0.341). This indicates that vegetation cover played an important role in the occurrence of soil erosion, which was consistent with the results of the one-way regression analysis. Among the socioeconomic factors, *Population* ∩ *GDP (*q value 0.246), *Population* ∩ *LUCC* (q value 0.308), and human activity factors all showed two-way interactions, but the change was small. No factor acted completely independently, indicating that the interaction of any two drivers had a greater effect on the occurrence of soil erosion in the study area than a single factor.

## 4. Discussion

### 4.1. Spatial and temporal evolution of soil erosion and the analysis of driving forces

The spatial and temporal succession of soil erosion in the eastern subtropical forest subregion of the Jiangnan Hills was analyzed over 20 years using the RUSLE model with 5-year intervals. The total amount and area of soil erosion significantly decreased over the study period. The erosion in the study area was dominated by micro erosion and slight erosion. Eroded areas graded intense and above mainly occurred in the center and southwest of the study area, which was consistent with the results of previous studies [51,52].

Soil erosion is the result of a combination of natural and socio-economic factors [53,54]. Regression and factor analyses were conducted to determine the role of typical factors (precipitation and vegetation). The results showed that the study area had abundant rainfall and the *R*-factor regression slope values were >0, generally consistent with previous studies [55]. , Interestingly the rainfall erosion force in the study area increased, but the erosion conditions improved. The decreasing trend of soil erosion intensity was obvious, which may be attributed to the policy guidelines of forestry reform, plain greening, and resource protection [24]. In terms of vegetation, 74.84% of the areas where the soil erosion intensity decreased spatially overlapped with areas where the *NDVI* increased significantly ($p < 0.01$). This suggests that increased vegetation cover reduced soil erosion in the region [56,57]. The factor detection results showed that the cause of soil erosion in this area was a combination of multiple factors, with vegetation playing an important role in regional soil erosion processes.

### 4.2. Effects of land use and slope gradient on soil erosion

Human activity and related land use changes were the primary causes of accelerated soil erosion [58], The area of micro erosion and slight erosion accounted for 70% in each land use type. Although the intensity of soil erosion in forest land areas continued to

**Table 4**
Factor detection results.

| Factor | NDVI | Slope | Slope direction | Temperatures | Precipitation | Elevation | Sandy soil | Clay | Powdered earth | Population density | GDP | Land Use |
|---|---|---|---|---|---|---|---|---|---|---|---|---|
| q-value | 0.235 | 0.073 | 0.238 | 0.211 | 0.251 | 0.143 | 0.216 | 0.219 | 0.225 | 0.242 | 0.241 | 0.269 |
| p-value | 0 | 0 | 0 | 0 | 0 | 0 | 0 | 0 | 0 | 0 | 0 | 0 |

Note: NDVI is annual vegetation cover, the temperature is the annual average temperature, precipitation is annual precipitation, and population density and GDP are 2015 statistics.

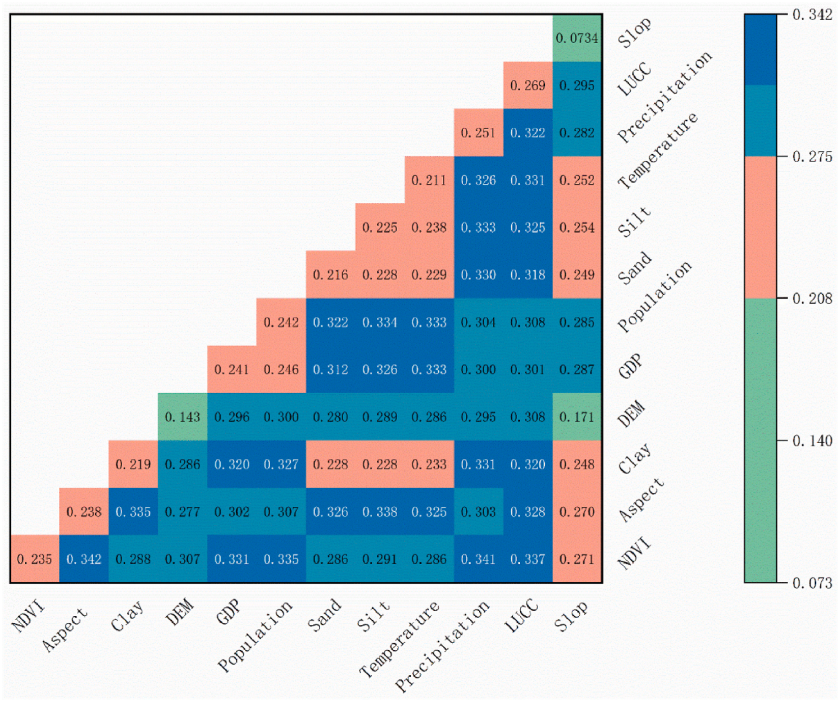


**Fig. 10.** Thermal map of interactive detection.
Note: The horizontal and vertical coordinates indicate the values of the two interacting factors, and the values indicate the magnitude of the interaction effect factor.

decline, forest land continued to have a high intensity of soil erosion. Typically, high vegetation cover favors the suppression of soil erosion [59]. This may be due to the high local rainfall, the single tree species structure of the secondary forest, the lack of understory vegetation, the splash effect [60], and the fragile red soil, resulting in forest runoff [61]. Forest land requires more attention for regional soil and water conservation, even though forest land erosion has lessened. Previous studies showed that the area of soil loss was proportional to the power of the slope [62,63]. For soils with runoff rates unaffected by slope length, there was a direct relationship between slope length and soil loss [64–66]. The interaction of different topographies, climate, soil types, and other factors can affect the soil erosion patterns in different regions. This study found that soil erosion intensity in regional cropland areas increased slowly in patches. Soil erosion decreased in the transition zone between arable land, towns, and forests. Existing experience has shown that measures such as straw mulching and terracing should be used to protect arable land ecology. Areas unsuitable for farming should be reforested and ecological compensation should be provided [67,68].

In terms of slope, the percentage of micro erosion area in all grades of slope exceeded 61% in the study, and the erosion grade was positively correlated with slope [69,70]. However, the degree of soil erosion restoration in the study area was not significantly related to slope. Erosion recovery was evident on slopes of 8–15°, whereas slopes >15° were areas of high erosion. By analyzing the land use types of steep slopes, the highest percentage of soil erosion area in forest land was found when the slope was >15°. The erosion intensity of cropland was higher than that of grassland, and the erosion area of cropland with a moderate grade and above was 34.13% higher than that of grassland. Previous studies have shown that sloping cropland is an important factor contributing to soil erosion in the red soil zone [71]. Tillage systems should be improved to reduce soil erosion on sloping cropland [72,73]. The rate of recovery of cropland erosion was greater than that of forest and grass over the 20 years (66.22%). This may be attributed to the reduction in the area of cultivated land on steep slopes in hilly areas due to China's Returning Farmland to Forest Program [74,75], as well as the improvement of farming systems in red soil areas [24].

### *4.3. Limitations of this study*

In this study, water erosion was estimated based on a time series in the study area, which has a subtropical monsoon climate with frequent short-term heavy rainfall. However, this study did not consider the effects of two key factors, heavy rainfall and storms [76,77]. The *R*-factor was calculated by the Zhang method based on the average annual precipitation and the results were stable in the same climate zone, but the results were large compared with the Naipal method [78]. The *P*-factor was not further refined due to the lack of real testing and the processing was not sufficiently detailed. It is necessary to further study the *P*-factor calculations.

The spatial distribution and development trend of soil erosion in the study area were consistent with the historical data from previous studies in the area [79,80], although the modeling factors involved some uncertainty. Despite the differences in the quantitative results, they did not affect the detailed analysis.

## 5. Conclusions

This study estimated soil erosion in the eastern subtropical forest subzone of the Jiangnan Hills from 2000 to 2020. The results of this study showed that the amount of soil erosion decreased by $3.96 \times 10^7$ t/a from 2000 to 2020, with the area and intensity of erosion reducing significantly. Due to natural and anthropogenic factors, the spatial distribution pattern of soil erosion in the study area had the characteristics of both local aggregation and local dispersion. The natural resource zoning could better represent this spatial pattern.

In this study 64.33% of the increased area of soil erosion was distributed in the arable area, and the decrease of *C*-factor values in the arable area tended to be equivalent to the increase trend in soil erosion. The vegetation cover of cultivated land was largely influenced by the tillage method and tillage density, and the management of soil erosion should consider the type and density of human activities on the relevant land types. Agricultural production on steep slopes with an average annual rainfall greater than 1000 mm should be avoided. Cultivation measures and ecological protection measures should be taken in the red soil zone to reduce the impact of soil erosion. The descriptions of soil and water conservation measure factors and the analysis of soil erosion time series deserve further study.

## Author contribution

Fuyin Guo; Xiaohuang Liu: Conceived and designed the experiments; Performed the experiments; Wrote the paper. Zulpiya Mamat; Wenbo Zhang: Conceived and designed the experiments; Contributed reagents, materials, analysis tools or data. Liyuan Xing; Ran Wang; Xinping Luo; Chao Wang; Honghui Zhao: Analyzed and interpreted the data.

## Funding statement

This study was supported by the Research on integrated technology system of natural resources observation and monitoring, No. DD20230514.

## Data availability statement

All required data and materials are included in the manuscript.

## Additional information

No additional information is available for this paper.

## Ethics declarations

Review and/or approval by an ethics committee was not needed for this study because this study has no ethical implications.

## Declaration of competing interest

The authors declare that they have no known competing financial interests or personal relationships that could have appeared to influence the work reported in this paper.

## Acknowledgements

Authors would like to thank the teachers at the Natural Resources Integrated Survey Command Center of the China Geological Survey for their guidance on the structure and writing of the paper and the teachers at Xinjiang University for their help.

## References

[1] G.h. Zhang, B.y. Liu, G.b. Liu, X.w. He, Detachment of undisturbed soil by shallow flow, Soil Sci. Soc. Am. J. 67 (2003) 713–719, https://doi.org/10.2136/sssaj2003.7130.
[2] H. Wang, J. Gao, W. Hou, Quantitative attribution analysis of soil erosion in different geomorphological types in karst areas: based on the geodetector method, J. Geogr. Sci. 29 (2019) 271–286, https://doi.org/10.1007/s11442-019-1596-z.
[3] B. Talukder, N. Ganguli, R. Matthew, G.W. vanLoon, K.W. Hipel, et al., Climate change-triggered land degradation and planetary health: a review, Land Degrad. Dev. 32 (2021) 4509–4522, https://doi.org/10.1002/ldr.4056.
[4] B. Liu, Y. Xie, Z. Li, Y. Liang, W. Zhang, et al., The assessment of soil loss by water erosion in China, Int. Soil Water Conserv. Res. 8 (2020) 430–439, https://doi.org/10.1016/j.iswcr.2020.07.002.
[5] B. Wang, X. Zhao, X. Wang, Z. Zhang, L. Yi, et al., Spatial and temporal variability of soil erosion in the black soil region of northeast China from 2000 to 2015, Environ. Monit. Assess. 192 (2020) 370, https://doi.org/10.1007/s10661-020-08298-y.
[6] Y. Kim, C.G. Kim, K.S. Lee, Y. Choung, Effects of post-fire vegetation recovery on soil erosion in vulnerable montane regions in a monsoon climate: a decade of monitoring, J. Plant Biol. 64 (2021) 123–133, https://doi.org/10.1007/s12374-020-09283-1.
[7] G. Qiankun, H. Yanfang, L. Baoyuan, Rates of soil erosion in China: a study based on runoff plot data, Catena 124 (2015) 68–76, https://doi.org/10.1016/j.catena.2014.08.013.

[8] W. Liu, M. Xing, Isotopic indicators of carbon and nitrogen cycles in river catchments during soil erosion in the arid loess plateau of China, Chem. Geol. 296–297 (2012) 66–72, https://doi.org/10.1016/j.chemgeo.2011.12.021.

[9] K. Sharma, S. Singh, Satellite remote sensing for soil erosion modelling using the answers model, Hydrol. Sci. J. 40 (1995) 259–272, https://doi.org/10.1080/02626669509491408.

[10] G. Pickup, V.H. Chewings, Forecasting patterns of soil erosion in arid lands from landsat mss data, Int. J. Rem. Sens. 9 (1988) 69–84, https://doi.org/10.1080/01431168808954837.

[11] S. Mohammed, M. Hussien, K. Alsafadi, A. Mokhtar, G. Rianna, et al., Assessing the wepp model performance for predicting daily runoff in three terrestrial ecosystems in western Syria, Heliyon 7 (2021), e06764, https://doi.org/10.1016/j.heliyon.2021.e06764.

[12] P.V.G. Batista, J. Davies, M.L.N. Silva, J.N. Quinton, On the evaluation of soil erosion models: are we doing enough? Earth Sci. Rev. 197 (2019), 102898 https://doi.org/10.1016/j.earscirev.2019.102898.

[13] K.M. Turnage, S.Y. Lee, J.E. Foss, K.H. Kim, I.L. Larsen, Comparison of soil erosion and deposition rates using radiocesium, rusle, and buried soils in dolines in east Tennessee, Environ. Geol. 29 (1997) 1–10, https://doi.org/10.1007/s002540050097.

[14] Changguang Wu, L. Sheng, R. Huadong, Y. Xiaohua, H. Zijie, Quantitative estimation of vegetation cover and management factor in usle and rusle models by using remote sensing data: a review, Chin. J. Appl. Ecol. 23 (6) (2012) 1728–1732, https://doi.org/10.13287/j.1001-9332.2012.0278.

[15] W. Qin, Q. Zhu, Y. Zhang, Soil erosion assessment of small watershed in loess plateau based on gis and rusle, Trans. Chin. Soc. Agric. Eng. 25 (2009) 157–163, https://doi.org/10.3969/j.issn.1002-6819.2009.08.029.

[16] L. Hongzhu, L. Lili, F. Tonggang, G. Hui, L. Min, et al., Vertical distribution of vegetation in mountain regions: a review based on bibliometrics, Chin. J. Eco-Agric. 30 (2022) 1077–1090, 10.3969/j.issn.1002-6819.2009.08.029.

[17] K. Li, L. Wang, Z. Wang, Y. Hu, Y. Zeng, et al., Multiple perspective accountings of cropland soil erosion in China reveal its complex connection with socioeconomic activities, Agric. Ecosyst. Environ. 337 (2022), 108083, https://doi.org/10.1016/j.agee.2022.108083.

[18] N. de Santos Loureiro, M. de Azevedo Coutinho, A new procedure to estimate the rusle ei30 index, based on monthly rainfall data and applied to the algarve region, Portugal, J. Hydrol. 250 (2001) 12–18, https://doi.org/10.1016/S0022-1694(01)00387-0.

[19] G. Zihan, C. Xiaohong, H. Yanhu, Spatiotemporal analysis of water resources system vulnerability in the lancang river basin, China, J. Hydrol. 601 (2021), 126614, https://doi.org/10.1016/j.jhydrol.2021.126614.

[20] B. Fu, W. Zhao, L. Chen, Q. Zhang, Y. Lü, et al., Assessment of soil erosion at large watershed scale using rusle and gis: a case study in the loess plateau of China, Land Degrad. Dev. 16 (2005) 73–85, https://doi.org/10.1002/ldr.646.

[21] C. Sixu, Y. Xiaohuan, X. Linlin, C. Hongyan, Study of soil erosion in the southern hillside area of China based on rusle model, Resour. Sci. 36 (2014) 1288–1297.

[22] Y. Liu, Y. Wang, Rural land engineering and poverty alleviation: lessons from typical regions in China, J. Geogr. Sci. 29 (2019) 643–657, https://doi.org/10.1007/s11442-019-1619-9.

[23] X. Wu, Z. Gu, Contribution weight of forest canopy and grass layers to soil and water conservation on water-eroded areas in southern China, Eurasian Soil Sci. 53 (2020) 1004–1012, https://doi.org/10.1134/S1064229320070169.

[24] L. Wang, H. Yan, X.W. Wang, Z. Wang, S.X. Yu, et al., The potential for soil erosion control associated with socio-economic development in the hilly red soil region, southern China, Catena 194 (2020), 104678, https://doi.org/10.1016/j.catena.2020.104678.

[25] Z. Haiyan, F. Jiangwen, H. Lin, T. Yulei, Y. Ying, et al., Theories and technical methods for the comprehensive regionalization of natural resources in China, Resour. Sci. 42 (2020) 1870–1882, https://doi.org/10.18402/resci.2020.10.05.

[26] F. Yujia, T. Changhai, L. Xiaohuang, S. Xingli, Y. Zemin, et al., Definition, classification, observation and monitoring of natural resources and their application in territoria, Chin. Geol. 49 (2022) 1048–1063, https://doi.org/10.12029/gc20220402.

[27] L.A.I. Ming, W.U. Shuyu, Z. Haiyan, L.I.U. Jiufen, W. Xinhua, et al., Analysis on the characteristics of natural resources dynamic changes in southwest China based on comprehensive regionalization, Geol. Surv. China (2021) 83–91, https://doi.org/10.19388/j.zgdzdc.2021.02.12.

[28] L. Jialei, S. Ranhao, X. Muqi, Y. Guocheng, Estimation of soil erosion based on the rusle model in China, Acta Ecol. Sin. 40 (2020) 3473–3485, https://doi.org/10.5846/stxb201903290610.

[29] W. Qin, Q. Guo, W. Cao, Z. Yin, Q. Yan, et al., A new rusle slope length factor and its application to soil erosion assessment in a loess plateau watershed, Soil Till. Res. 182 (2018) 10–24, https://doi.org/10.1016/j.still.2018.04.004.

[30] O. Baskan, Analysis of spatial and temporal changes of rusle-k soil erodibility factor in semi-arid areas in two different periods by conditional simulation, Arch. Agron Soil Sci. 68 (2022) 1698–1710, https://doi.org/10.1080/03650340.2021.1922673.

[31] A.O. Pinson, J. S, J. A, a.S. AuBuchon, A new method for calculating c factor when projecting future soil loss using the revised universal soil loss equation (rusle) in semi-arid environments, Catena (2023), https://doi.org/10.1016/j.catena.2023.107067.

[32] K. Renard, G. Foster, G. Weesies, D. McCool, D. Yoder, et al., Predicting Soil Erosion by Water:A Guide to Conservation Planning with the Revised Universal Soil Loss Equation (Rusle), AGR HANDB, 1997. https://handle.nal.usda.gov/10113/11126.

[33] L. Jingfang, H. Feinan, X. Chenyang, D. Wei, Y. Zhenghong, et al., Specific ion effects on soil aggregate stability and rainfall splash erosion, Int. Soil Water Conserv. Res. 10 (2022) 557–564, https://doi.org/10.1016/j.iswcr.2022.02.001.

[34] Z. wenbo, F. jinsheng, Rainfall erosivity estimation under different rainfall amount, Resour. Sci. 25 (2003) 35–41, 10.3321/j.issn:1007-7588.2003.01.006.

[35] H. Yan, L. Wang, T.W. Wang, Z. Wang, Z.H. Shi, A synthesized approach for estimating the c-factor of rusle for a mixed-landscape watershed: a case study in the gongshui watershed, southern China, Agric. Ecosyst. Environ. 301 (2020), 107009, https://doi.org/10.1016/j.agee.2020.107009.

[36] F. Jin, W. Yang, J. Fu, S. Z. J, T. o, T.E. Li, Effects of vegetation and climate on the changes of soil erosion in the loess plateau of China, Sci. Total Environ. 773 (2021), 145514, https://doi.org/10.1016/j.scitotenv.2021.145514.

[37] A. Almagro, T.C. Thomé, C.B. Colman, R.B. Pereira, J.M. Junior, et al., Improving cover and management factor (c-factor) estimation using remote sensing approaches for tropical regions, Int. Soil Water Conserv. Res. 7 (2019) 325–334, https://doi.org/10.1016/j.iswcr.2019.08.005.

[38] D. Andreatta, D. Gianelle, M. Scotton, M.J.E.I. Dalponte, Estimating grassland vegetation cover with remote sensing: a comparison between landsat-8, sentinel-2 and planetscope imagery, Ecol. Indicat. 141 (2022), 109102, https://doi.org/10.5846/stxb201903290610.

[39] P. Tian, Z. Zhu, Q. Yue, Y. He, Z. Zhang, et al., Soil erosion assessment by rusle with improved p factor and its validation: case study on mountainous and hilly areas of hubei province, China, Int. Soil Water Conserv. Res. 9 (2021) 433–444, https://doi.org/10.1016/j.iswcr.2021.04.007.

[40] C. Alewell, P. Borrelli, K. Meusburger, P. Panagos, Using the usle: chances, challenges and limitations of soil erosion modelling, Int. Soil Water Conserv. Res. 7 (2019) 203–225, https://doi.org/10.1016/j.iswcr.2019.05.004.

[41] Z. Jianlin, Y. Zhiqiang, G. Gerard, Soil and water conservation measures reduce soil and water losses in China but not down to background levels: evidence from erosion plot data, Geoderma 337 (2019) 729–741, https://doi.org/10.1016/j.geoderma.2018.10.023.

[42] S. Schmidt, S. Tresch, K.J.M. Meusburger, Modification of the rusle slope length and steepness factor (ls-factor) based on rainfall experiments at steep alpine grasslands, MethodsX 6 (2019) 219–229, https://doi.org/10.1016/j.mex.2019.01.004.

[43] T. Gashaw, A.W. Worqlul, Y.T. Dile, S. Addisu, A. Bantider, et al., Evaluating potential impacts of land management practices on soil erosion in the gilgel abay watershed, upper blue nile basin, Heliyon 6 (2020), e04777, https://doi.org/10.1016/j.heliyon.2020.e04777.

[44] L. Ao, Z.X. John, L. Baoyuan, Effects of dem resolutions on soil erosion prediction using Chinese soil loss equation, Geomorphology 384 (2021), 107706, https://doi.org/10.1016/j.geomorph.2021.107706.

[45] B. Liu, K. Zhang, J. Jiao, Soil erodibility and its use in soil erosion prediction model, J. Nat. Resour. 14 (1999) 345–350, https://doi.org/10.3321/j.issn:1000-3037.1999.04.010.

[46] J. Williams, K. Renard, P. Dyke, Epic: a new method for assessing erosion's effects on soil productivity, J. Soil Water Conserv. 38 (1983) 381–383.

[47] C. JiLin, C. Li, F. XiangJing, Soil erosion characteristics of different slope gradients and aspects in songhuaba watershed of kunming, J. W. China Forest. Sci. 41 (2012) 63–67, https://doi.org/10.16473/j.cnki.xblykx1972.2012.06.003.

[48] X. Zhou, H. Wen, Y. Zhang, J. Xu, W. Zhang, Landslide susceptibility mapping using hybrid random forest with geodetector and rfe for factor optimization, Geosci, Front. Times 12 (2021), 101211, https://doi.org/10.1016/j.gsf.2021.101211.

[49] W. Jinfeng, X. Chengdong, Geodetector: principle and prospective, Acta Geograph. Sin. 72 (2017) 116–134, https://doi.org/10.11821/dlxb201701010.
[50] J.F. Wang, X.H. Li, G. Christakos, Y.L. Liao, T. Zhang, et al., Geographical detectors-based health risk assessment and its application in the neural tube defects study of the heshun region, China, Int. J. Geogr. Inf. Sci. 24 (2010) 107–127, https://doi.org/10.1080/13658810802443457.
[51] X. Liu, Y. Bao, Y. Wang, D. Zhang, M. Hu, et al., Spatiotemporal variation characteristics of sediment nutrient load from the soil erosion of the yangtze river basin of China from 1901 to 2010, Ecol. Indicat. 150 (2023), 110206, https://doi.org/10.1016/j.ecolind.2023.110206.
[52] T. Hongfen, H. Jie, Z. Yue, Z. Lian-qing, S. Zhou, Modelling and mapping soil erosion potential in China, J. Integr. Agric. 18 (2019) 251–264, https://doi.org/10.1016/S2095-3119(18)62045-3.
[53] Z. Wang, Y. Zeng, C. Li, H. Yan, S. Yu, et al., Telecoupling cropland soil erosion with distant drivers within China, J. Environ. Manag. 288 (2021), 112395, https://doi.org/10.1016/j.jenvman.2021.112395.
[54] C. Xiaoan, L. Ziwei, Z. Zhanyu, Z. Long, Effects of soil and water conservation measures on runoff and sediment yield in red soil slope farmland under natural rainfall, Sustainability 12 (2020) 3417, https://doi.org/10.3390/su12083417.
[55] J. Zhou, B. Fu, G. Gao, Y. Lü, Y. Liu, et al., Effects of precipitation and restoration vegetation on soil erosion in a semi-arid environment in the loess plateau, China, Catena 137 (2016) 1–11, https://doi.org/10.1016/j.catena.2015.08.015.
[56] J. Huo, C. Liu, X. Yu, L. Chen, W. Zheng, et al., Direct and indirect effects of rainfall and vegetation coverage on runoff, soil loss, and nutrient loss in a semi-humid climate, Hydrol. Process. 35 (2021), e13985, https://doi.org/10.1002/hyp.13985.
[57] C. Jia, X. Haibing, L. Zhongwu, L. Cheng, W. Danyang, et al., Threshold effects of vegetation coverage on soil erosion control in small watersheds of the red soil hilly region in China, Ecol. Eng. 132 (2019) 109–114, https://doi.org/10.1016/j.ecoleng.2019.04.010.
[58] P. Borrelli, D.A. Robinson, L.R. Fleischer, E. Lugato, C. Ballabio, et al., An assessment of the global impact of 21st century land use change on soil erosion, Nat. Commun. 8 (2017) 2013, https://doi.org/10.1038/s41467-017-02142-7.
[59] C. Jia, L. Zhongwu, X. Haibing, N. Ke, T. Chongjun, Effects of land use and land cover on soil erosion control in southern China: implications from a systematic quantitative review, J. Environ. Manag. 282 (2021), 111924, https://doi.org/10.1016/j.jenvman.2020.111924.
[60] L. Yaojun, Y. Guangyong, X. Mingze, T. Chongjun, Y. Jie, Splash erosion features of three red soils in poyang lake basin, J. Soil Water Conserv. 33 (2019) 55–59 +67, https://doi.org/10.13870/j.cnki.stbcxb.2019.02.009.
[61] J. Q.-G, B.o.S. Zhao, W. Conservation, Some considerations for present soil and water conservation and ecology security of south China, Bull. Soil Water Conserv. 26 (2006) 1–8, https://doi.org/10.1016/S1872-2032(06)60050-4.
[62] C. Tao, S. Jisen, H. Liu, T. Guang, Y. Guoyu, et al., Modeling the effects of topography and slope gradient of an artificially formed slope on runoff, sediment yield, water and soil loss of sandy soil, Catena 212 (2022), 106060, https://doi.org/10.1016/j.catena.2022.106060.
[63] R. Chakrabortty, S.C. Pal, M. Sahana, A. Mondal, J. Dou, et al., Soil erosion potential hotspot zone identification using machine learning and statistical approaches in eastern India, nat. Hazard. Rev. 104 (2020) 1259–1294, https://doi.org/10.1007/s11069-020-04213-3.
[64] G. Jordan, A.v. Rompaey, P. Szilassi, G. Csillag, C. Mannaerts, et al., Historical land use changes and their impact on sediment fluxes in the balaton basin (Hungary), Agric. Ecosyst. Environ. 108 (2005) 119–133, https://doi.org/10.1016/j.agee.2005.01.013.
[65] M. Li, X. Shi, Z. Shen, E. Yang, H. Bao, et al., Effect of hillslope aspect on landform characteristics and erosion rates, Environ. Monit. Assess. 191 (2019) 598, https://doi.org/10.1007/s10661-019-7760-1.
[66] B. Zhu, Z. Zhou, Z. Li, Soil erosion and controls in the slope-gully system of the loess plateau of China: a review, Front. Environ. Sci. 9 (2021), https://doi.org/10.3389/fenvs.2021.657030.
[67] D. Cuiting, L. Yaojun, W. Tianwei, L. Zhaoxia, Z. Yiwen, Exploring optimal measures to reduce soil erosion and nutrient losses in southern China, Agric. Water Manag. 210 (2018) 41–48, https://doi.org/10.1016/j.agwat.2018.07.032.
[68] L. Gutiérrez Rodríguez, N.J. Hogarth, Z. Wen, X. Chen, Z. Kun, et al., China's conversion of cropland to forest program: a systematic review of the environmental and socioeconomic effects, Environ. Evid. 5 (2016) 21, https://doi.org/10.1186/s13750-016-0071-x.
[69] X. Yueqing, F. Yan, Z. Dong, G. Feige, Soil erosion dynamics in maotiao river watershed of guizhou province, Bull. Soil Water Conserv. 31 (2011) 186–190, https://doi.org/10.13961/j.cnki.stbctb.2011.01.035.
[70] C. Lin, S. Tiancheng, W. Tianwei, L. Zhaoxia, C. Chongfa, Temporal and spatial heterogeneity of soil erosion and a quantitative analysis of its determinants in the three gorges reservoir area, China, Int. J. Environ. Res. Publ. Health 17 (2020) 8486, https://doi.org/10.3390/ijerph17228486.
[71] C. Longxi, Z. Yugang, L. Huizhong, Y. Jiuqin, Z. Yayun, et al., Grass hedge effects on controlling soil loss from concentrated flow: a case study in the red soil region of China, Soil Till. Res. 148 (2015) 97–105, https://doi.org/10.1016/j.still.2014.12.009.
[72] Y. Ma, Z. Li, C. Deng, J. Yang, C. Tang, et al., Effects of tillage-induced soil surface roughness on the generation of surface–subsurface flow and soil loss in the red soil sloping farmland of southern China, Catena 213 (2022), 106230, https://doi.org/10.1016/j.catena.2022.106230.
[73] X. Haichao, Z. Jianhui, D. Jiadong, W. Yong, Review and prospect of tillage erosion research, Adv. Earth Sci. 34 (2019) 1288.
[74] Y. Zhang, D. Guan, L. Wu, X. Su, L. Zhou, et al., How can an ecological compensation threshold be determined? A discriminant model integrating the minimum data approach and the most appropriate land use scenarios, Sci. Total Environ. 852 (2022), 158377, https://doi.org/10.1016/j.scitotenv.2022.158377.
[75] Y. Zhou, X. Li, Y. Liu, Land use change and driving factors in rural China during the period 1995-2015, Land Use Pol. 99 (2020), 105048, https://doi.org/10.1016/j.landusepol.2020.105048.
[76] D. Jian, L. YaoJun, Y. Jie, T. ChongJun, S. ZhiHua, Role of groundcover management in controlling soil erosion under extreme rainfall in citrus orchards of southern China, J. Hydrol. 582 (2020), 124290, https://doi.org/10.1016/j.jhydrol.2019.124290.
[77] M.A. Mohamadi, A. Kavian, Effects of rainfall patterns on runoff and soil erosion in field plots, Int. Soil Water Conserv. Res. 3 (2015) 273–281, https://doi.org/10.1016/j.iswcr.2015.10.001.
[78] V. Naipal, C. Reick, J. Pongratz, K.J.G.M.D. Van Oost, Improving the global applicability of the rusle model–adjustment of the topographical and rainfall erosivity factors, Geosci. Model Dev. (GMD) 8 (2015) 2893–2913, https://doi.org/10.5194/gmd-8-2893-2015.
[79] Z. Li, K. Ning, J. Chen, C. Liu, D. Wang, et al., Soil and water conservation effects driven by the implementation of ecological restoration projects: evidence from the red soil hilly region of China in the last three decades, J. Clean. Prod. 260 (2020), https://doi.org/10.1016/j.jclepro.2020.121109.
[80] C. Jia, X. Haibing, L. Zhongwu, L. Cheng, N. Ke, et al., How effective are soil and water conservation measures (swcms) in reducing soil and water losses in the red soil hilly region of China? A meta-analysis of field plot data, Sci. Total Environ. 735 (2020), 139517, https://doi.org/10.1016/j.scitotenv.2020.139517.